Volatility of unevenly sampled fractional Brownian motion: An application to ice core records

Jörn Davidsen*
Complexity Science Group, Department of Physics & Astronomy, University of Calgary, Calgary, Alberta, Canada T2N 1N4 and British Antarctic Survey, Cambridge CB3 0ET, United Kingdom

James Griffin
British Antarctic Survey, Cambridge CB3 0ET, United Kingdom

(Received 12 June 2009; revised manuscript received 19 November 2009; published 21 January 2010)

The analysis of many natural time series and especially those related to ice core records often suffers from uneven sampling intervals. For fractional Brownian motion, we show that standard estimates of the volatility can be strongly biased due to uneven sampling. Taking these limitations into account, we study high-resolution records of temperature proxies obtained from Antarctic ice cores. We find that the volatility properties reveal a strong nonlinear component in the temperature time series for time scales of 5–200 kyr extending earlier results. These findings suggest in particular that temperature increments over these time scales appear in clusters of big and small increments—a big (positive or negative) change is most likely followed by a big (positive or negative) change and a small change is most likely followed by a small change.

DOI: 10.1103/PhysRevE.81.016107 PACS number(s): 89.90.+n, 05.45.Tp, 05.10.Gg, 92.40.Vq

I. INTRODUCTION

Techniques based on linear and nonlinear time series analyses are powerful tools to gain insight into the dynamics and properties of many natural systems [1–3]. While the mathematical foundations of many of these methods are well established for evenly sampled time series, this is generally not the case if the time interval between subsequent data points varies [4,5]. Notable exceptions include the well-known Lomb-Scargle periodogram [6,7] and related spectral estimates [8]. This is, however, only a very small subset of methods. Instead, a typical approach to unevenly sampled time series is, first, to use a more or less arbitrary interpolation scheme to generate an evenly sampled series from the recorded time series and then apply methods established for constant sampling frequencies. The effect and bias induced by such interpolation schemes on the used method are rarely addressed—see Refs. [9–12] for exceptions—often leaving substantial doubts on the obtained results and interpretations.

A particularly striking example of unevenly sampled time series are those derived from ice cores. Chemical concentrations and isotope ratios of the ice as well as greenhouse gas concentrations in the trapped air bubbles are measured as functions of depth [13–20]. Obviously, depth corresponds to time, yet the relation is highly nonlinear and contains significant trends due to the ice flow: most of the past is covered by the bottom part of an ice core. For instance, some of the oldest available ice cores—the Vostok core [13] and the European Project for Ice Coring in Antarctica (EPICA) dome C core [15,19], both from Antarctica—extend over more than 3000 m in depth and cover the last 422 and 802 kyr, respectively. Yet, the upper 1500 m correspond only to roughly 100 and 150 kyr, respectively. Consequently, the ice core records which are evenly sampled with respect to depth correspond to unevenly sampled time series.

In this paper, we study the effect of such a transformation on fractional Brownian motion (FBM)—a paradigmatic example of processes with long-range correlations which are typically thought to be relevant in the context of many natural systems including but not limited to climate dynamics [21–28]. We focus in particular on correlations in the volatility which have been used recently to distinguish between linear and nonlinear processes in the climate system [29–34] and play an important role in finance, as well [35]. To be specific, we simulate different types of FBM with annual resolution and apply the same measurement intervals as obtained for the Vostok ice core [13]. Then, we apply a straightforward resampling technique to obtain evenly sampled time series again, resembling the typical approach to unevenly sampled time series. The properties of these time series are compared to those of the directly measured FBM process. We find that the Vostok sampling intervals induce significant biases in the estimates of the volatility correlations for resolutions of less than 500 yr. For example, the exponent describing the linear two-point correlations in the volatility as measured by detrended fluctuation analysis (DFA) is significantly underestimated. We then introduce a simple method that allows one to reliably estimate the volatility properties of FBM despite uneven sampling.

Finally, to test claims that climate variations are nonlinear for time scales of 1–100 kyr [31] we reanalyze the volatility properties of the hydrogen isotope ratios (δD_{ice}) record from the Vostok core [13] and compare them to those of the recently published δD_{ice} record from the EPICA dome C (EDC) core [19], which extends much further back in time. We find nontrivial behavior in both cases indicating that a strong nonlinear component exists for time scales of 5–200 kyr. Our findings confirm in particular that temperature increments over these time scales appear in clusters of big and small increments—a big (positive or negative) change is most likely followed by a big (positive or negative) change and a small change is most likely followed by a small change.

*davidsen@phas.ucalgary.ca

 ©2010 The American Physical Society

The outline of the paper is as follows. In Sec. II, we introduce fractional Brownian motion and review its volatility properties. We also discuss how the uneven sampling based on the Vostok record, and the resampling, is implemented. In Sec. III, we briefly review detrended fluctuation analysis. The results for unevenly sampled fractional Brownian motion are given in Sec. IV and a method that corrects for the biases induced by the uneven sampling is discussed in Sec. V. In Secs. VI and VII, we present the results for the Vostok ice core and the EPICA dome C ice core, respectively. We close with a brief discussion in Sec. VIII.

II. FRACTIONAL BROWNIAN MOTION

Normalized fractional Brownian motion is a continuous-time real-valued Gaussian process $B_H(t)$ on $[0,T]$, with $T \in \mathbb{R}^{>0}$, starting at zero with mean zero and (linear) two-point correlation function

$$\langle B_H(t)B_H(s)\rangle = \tfrac{1}{2}(t^{2H} + s^{2H} - |t-s|^{2H}), \tag{1}$$

where $0<H<1$ is the Hurst exponent and $\langle\cdots\rangle$ represents the ensemble average [36]. For $H=1/2$, normal Brownian motion is recovered. Note that FBM is H self-similar with stationary increments. Since FBM is uniquely defined by the probability density function of its increments—a Gaussian (normal) distribution—and its two-point correlation function for a given value of the exponent H, all higher-order q-point correlation functions are fully determined by Eq. (1). Thus, FBM is indeed a *linear* stochastic process [2,5]. In contrast, a *nonlinear* stochastic process has nontrivial higher-order q-point correlation functions, i.e., knowledge of the distribution of the increments and of the two-point correlation function is not sufficient to specify the process.

The particular focus of this paper is on the volatility series of FBM, which is defined as

$$u_i^2 = [B_H(t_{i+1}) - B_H(t_i)]^2, \tag{2}$$

where $\{t_i\}$ is the set of discrete equidistant sampling times. Hence, the volatility characterizes the absolute size or magnitude of changes from one time step to the next, but it neglects any information about the sign of the changes. The properties of the volatility series have been used recently to distinguish between linear and nonlinear processes [29]. For FBM an analytical relation between the two-point correlation functions of $B_H(t)$ given in Eq. (1) and that of u_i^2 was derived in Ref. [33]. In particular, it was shown that the volatility series also has a two-point correlation function which can be characterized by a single exponent $\alpha_V(H)$. Its value is asymptotically given by $\alpha_V(H)=0.5$ for $0<H<0.75$ and $\alpha_V(H)=2H-1$ for $0.75<H<1$ [37]. However, the influence of nonequidistant sampling on estimating this exponent has not been investigated despite its direct relevance for the analysis of ice core records as studied, for example, in Ref. [31].

Here, we use the sampling intervals from the Vostok ice core [13] as shown in Fig. 1 to address this issue. It is important to note that typically each data point obtained from an ice core corresponds to an *average value* over a certain time interval, the so-called bag average. This is due to the measurement process which involves analyzing chemical or greenhouse gas concentrations or isotope ratios in a volume of ice that has accumulated over a certain time interval. Thus, in a first step we convert each discrete realization of FBM $B_H(t_i)$ with $1\le i\le 422\,766$ and $\{t_i\}=\{1,2,\ldots,422\,766\}$ into a series of unequally sampled bag averages $B_H^V(t_j)$, where the set $\{t_j\}$ and the intervals for the averaging are given by Fig. 1 (in years). This mimics the measurement process for the Vostok ice core and will be denoted the Vostok filter in the following. In a second step, this filtered series is used to generate an evenly sampled series of resolution R, $B_H^{V,R}(t_k)$, resembling the typical approach to unevenly sampled time series. Taking into account the nature of the bag averages, we use a simple resampling technique where we specify a given resolution R and perform a weighted average over each bag or bin of length R based on the recorded values. The weights are assigned according to the time interval covered by a given measurement value within a specific bin. Note that recorded values can contribute to more than one bin. The advantage of this resampling method is that it does not make any assumptions about the underlying process and it is purely based on the measured data.

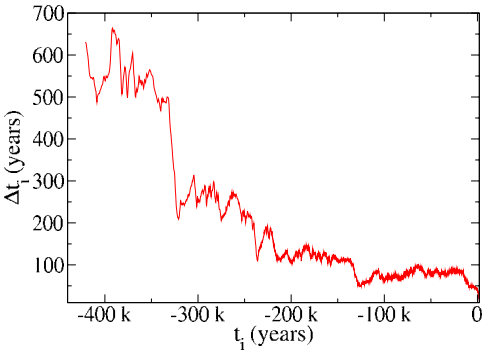

FIG. 1. (Color online) Time intervals $\Delta t_i = t_{i+1} - t_i$ between subsequent data points as a function of time t_i for the Vostok ice core. The data set contains 3311 points and covers 422 kyr.

III. DETRENDED FLUCTUATION ANALYSIS

In order to study the effect of the Vostok filter on the power-law correlations of the volatility series, we estimate the exponent $\alpha_V(H)$ using DFA [38,39]. This is exactly the same method applied in Refs. [31,32] to study the volatility correlations in isotope records obtained from different ice cores including the Vostok ice core.

To define DFA, let us consider a time series $(y_i)_{1\le i\le N}$ with zero mean $\langle y_i\rangle_i = 0$. For a fixed $n<N$, the series is divided into $N_n=[N/n]$ sections of size n. In each section the local trend is calculated by a least-squares fit. For DFAd, this trend is considered to be a polynomial of order d. Subtracting this local trend yields the detrended series,

$$Y_n(i) = y_i - y_{\mathrm{fit},n}(i). \tag{3}$$

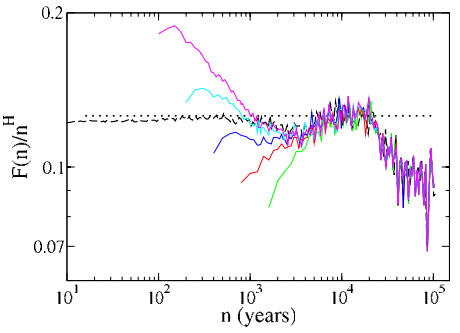

FIG. 2. (Color online) Rescaled DFA1 for a single realization of FBM with $H=0.8$ (dashed line) and the derived $B_{0.8}^{V,R}(t_k)$ for different resolutions R (solid lines): $R=25$, 50, 100, 200, 400 yr, from top to bottom. The expected asymptotic behavior is a flat curve as highlighted by the dotted line.

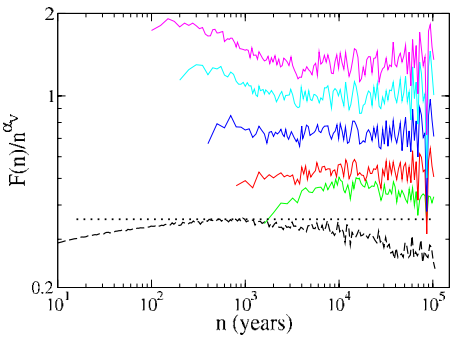

FIG. 3. (Color online) Rescaled DFA1 for the volatility series of a single realization of FBM with $H=0.8$ (dashed line) and of the derived $B_{0.8}^{V,R}(t_k)$ for different resolutions R (solid lines): $R=25$, 50, 100, 200, 400 yr, from top to bottom. The expected asymptotic behavior is a flat curve as highlighted by the dotted line which corresponds to $\alpha_V=2H-1=0.6$. The curves for $B_{0.8}^{V,R}(t_k)$ are shifted vertically for clarity.

The fluctuation function can then be calculated by

$$F(n)=\left(\frac{1}{nN_n}\sum_{i=1}^{nN_n}Y_n^2(i)\right)^{1/2}. \tag{4}$$

If the series $(y_i)_{1\le i\le N}$ is long-range correlated, the fluctuation function increases by a power law

$$F(n)\propto n^{\alpha}. \tag{5}$$

If $y_i=B_H(t_i)$, $\alpha=H$. In the case of the volatility series, $y_i=\Sigma_{j=0}^{i}u_j^2$ and $\alpha=\alpha_V$.

IV. RESULTS FOR FRACTIONAL BROWNIAN MOTION

Figure 2 shows the results of DFA for a single realization $B_{0.8}(t_i)$ with annual resolution. Indeed, $\alpha=H$ is recovered—the small deviations in $F(n)$ for large n are due to poor statistics. The fluctuation functions of $B_{0.8}^{V,R}(t_k)$ with $R=100$, 200, and 400 yr, respectively, are basically identical to those of $B_{0.8}(t_i)$. The deviations for small n are expected since they are intrinsic to the DFA method [39]. However, for $R\le 50$ yr pronounced nontrivial deviations in $F(n)$ are present for $n<1000$ yr. This agrees with a rough estimate based on

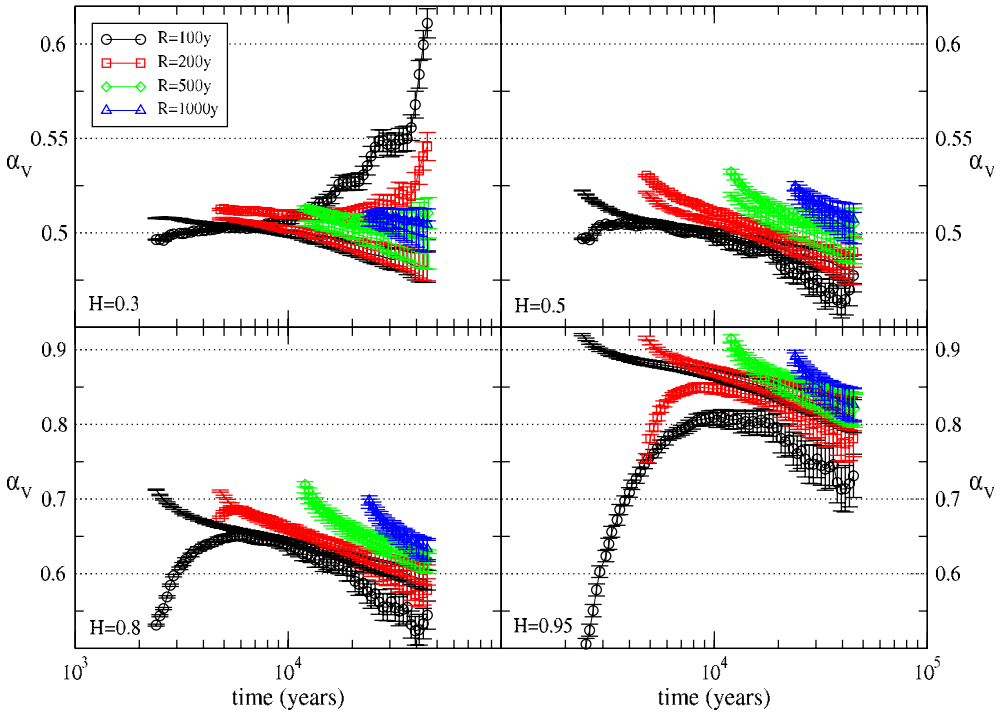

FIG. 4. (Color online) Local exponents α_V of the FBM volatility series with $H=0.3$, 0.5, 0.8, and 0.95 for different resolutions R. One-σ error bars are given. The lines with symbols correspond to the case of the Vostok filter $[B_H^{R,V}(t_k)]$, while the lines without symbols correspond to the directly and evenly sampled case $[B_H^R(t_k)]$. There are clear differences between the two cases for resolutions finer than 500 yr. Note the different scales for the two rows.

TABLE I. Summary of global estimates for α_V over the different ensembles of FBM obtained by DFA1. Each first entry corresponds to $B_H^{R,V}(t_k)$ while the second one corresponds to $B_H^R(t_k)$.

	$H=0.3$	$H=0.5$	$H=0.8$	$H=0.95$
$R=100$ yr	0.52 ± 0.03 (0.50 ± 0.03)	0.49 ± 0.03 (0.50 ± 0.03)	0.59 ± 0.05 (0.65 ± 0.05)	0.71 ± 0.06 (0.87 ± 0.06)
$R=200$ yr	0.52 ± 0.03 (0.50 ± 0.03)	0.51 ± 0.03 (0.50 ± 0.03)	0.64 ± 0.06 (0.65 ± 0.05)	0.80 ± 0.07 (0.87 ± 0.07)
$R=500$ yr	0.51 ± 0.04 (0.50 ± 0.04)	0.52 ± 0.04 (0.51 ± 0.04)	0.67 ± 0.07 (0.66 ± 0.07)	0.87 ± 0.08 (0.86 ± 0.08)
$R=1000$ yr	0.51 ± 0.05 (0.50 ± 0.05)	0.52 ± 0.05 (0.51 ± 0.05)	0.67 ± 0.08 (0.67 ± 0.08)	0.87 ± 0.1 (0.86 ± 0.1)

Fig. 1, which suggests nontrivial deviations for $n<700$ yr. Thus, Fig. 2 indicates that the estimate of H using DFA is not significantly influenced by the uneven sampling associated with the Vostok filter if either the resolution is larger than approximately 100 yr or only time scales larger than approximately 1000 yr are considered. This is confirmed by a systematic statistical analysis [40].

However, the situation is different for the volatility series. As discussed in Ref. [33], the estimate of α_V suffers from strong finite-size effects. This is directly reflected in Fig. 3, which shows systematic deviations from the expected asymptotic behavior for a single realization $B_{0.8}(t_i)$ with annual resolution. Moreover, the fluctuation functions for the volatility series of $B_{0.8}^{V,R}(t_k)$ with $R=25$, 50, 100, 200, and 400 yr, respectively, seem to behave differently even for large n.

To investigate this systematically, we consider ensembles of 1000 realizations of FBM for different values of H. For each ensemble, we compute the average α_V and estimate its standard error [41]. In particular, we compare the results for $B_H^{R,V}(t_k)$ with those for $B_H^R(t_k)$ where the latter corresponds to the resampled series in the absence of the Vostok filter. To take into account the apparent variability of α_V over different intervals of n (see Fig. 3), we compute α_V for sliding windows spanning slightly less than an order of magnitude in n similar to the approach in Ref. [42]. The averages of these local slopes are shown in Fig. 4. Obviously, there are clear statistical differences between $B_H^{R,V}(t_k)$ and $B_H^R(t_k)$ for $R<500$ yr. In contrast to the estimate of H (see Fig. 2), these differences often even persist on large time scales, namely, $n>1000$ yr.

As Table I shows, these differences are not as obvious if one only considers the global estimates of α_V. However, it is clear in both cases that the differences are more pronounced for $H\to 1$.

While FBM is a linear stochastic process, we also find that estimates of the volatility properties of nonlinear time series generated by a variant of the multiplicative random cascade process [43] are severely biased for small resolutions R due to the Vostok filter. This indicates that this phenomenon is not restricted to linear processes and indeed of rather general nature.

V. CORRECTION METHOD

To correct for the bias induced by the Vostok filter, we introduce a modified volatility series. One of the main effects of the varying time intervals associated with the bag averages is to render the variance between subsequent measurement values inhomogeneous. To compensate for this, we define

$$\hat{u}_j^2 = \frac{[B_H^V(t_{j+1}) - B_H^V(t_j)]^2}{\mathrm{var}[B_H^V(t_{j+1}) - B_H^V(t_j)]}. \tag{6}$$

For an evenly sampled time series, $\mathrm{var}[B_H^V(t_{j+1})-B_H^V(t_j)]$ would be constant. For an unevenly sampled time series, however, it typically fluctuates. One can easily compute the variance (see the Appendix for details) and it is given by

$$\mathrm{var}[B_H^V(t_{j+1}) - B_H^V(t_j)] = \int_0^{m+n} h(\tau)c(\tau)d\tau. \tag{7}$$

Here, $m=t_{j+1}-t_j$, $n=t_{j+2}-t_{j+1}$, $c(\tau)$ is the two-point correlation function of the *increments* of FBM, and the function h is given by

$$h(\tau) = \begin{cases} \dfrac{(n+m-\tau^3)}{12mn} + \dfrac{(n+m)(\tau-n)^3}{12mn^2} + \dfrac{(n+m)(\tau-m)^3}{12m^2n} & \text{for } 0\le\tau\le n,m \\ \dfrac{(n+m-\tau)^3}{12mn} + \dfrac{(n+m)(\tau-n)^3}{12mn^2} & \text{for } m\le\tau\le n \\ \dfrac{(n+m-\tau)^3}{12mn} + \dfrac{(n+m)(\tau-m)^3}{12m^2n} & \text{for } n\le\tau\le m \\ \dfrac{(n+m-\tau)^3}{12mn} & \text{for } n,m\le\tau\le n+m. \end{cases} \tag{8}$$

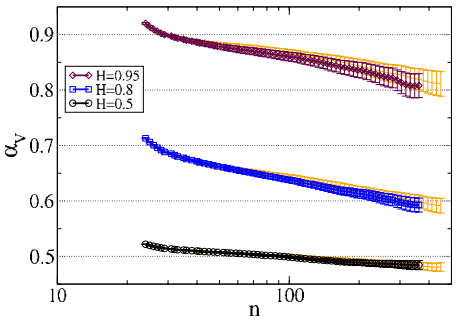

FIG. 5. (Color online) Local exponents α_V estimated from the modified volatility series as defined in Eqs. (6) and (9) for different values of H (lines with symbols). One-σ error bars are given. The (orange) lines without symbols show the local exponents α_V for $B_H^{100}(t_k)$ (H=0.95, 0.8, 0.5 from top to bottom) for comparison because of their similar length.

Note that $c(\tau) \propto |\tau|^{2H-2}$ for $H \neq 0.5$ and $c(\tau) = \delta(\tau)$ for $H = 1/2$ [24,44]. As shown in the Appendix, in the special case $n=m$, Eq. (7) reduces to the expected scaling

$$\mathrm{var}[B_H^V(t_{j+1}) - B_H^V(t_j)] \propto m^{2H}, \tag{9}$$

which is also a good approximation for $|n-m| \ll m/(2-H)$. Since $|n-m| < m/10$ for all j of the Vostok filter, this is the relevant case here and Eq. (9) will be used in the following. Note that for other unevenly sampled data sets this approximation might not be suitable in which case Eq. (7) has to be evaluated explicitly. Some special cases are discussed in the Appendix.

Figure 5 shows the estimates for α_V for the modified volatility series given by Eq. (6). Clearly, the behavior of the directly and evenly sampled case $B_H^R(t_k)$ is recovered. Thus, the modified volatility series allows one to reliably estimate α_V for FBM despite the uneven sampling.

VI. RESULTS FOR VOSTOK ICE CORE

The results presented above suggest that one should either consider resolutions $R \geq 500$ yr (Sec. IV) or use the correction method given in Sec. V to obtain reliable estimates for the volatility properties of data from the Vostok ice core. Here, we will focus on the hydrogen isotope ratio of the ice, δD_{ice}, which is a proxy for the surface temperature at the time when the ice was formed and, hence, typically used to reconstruct the global climate [13]. As for FBM, we find that the fluctuation function of the volatility series strongly varies with the chosen resolution—see the inset of Fig. 6. These variations are even more pronounced if one tries to fit local exponents α_V as shown in the main panel of Fig. 6. Comparing the results for FBM (see Fig. 4 and Table I) to the strong variation in α_V with R for the Vostok data suggests that the uneven sampling is not solely responsible for the variation. In particular, we would expect very similar behavior for R = 500 and 1000 yr based on the results for FBM. Thus, the significant difference in α_V between R=500 and 1000 yr is surprising and implies that one should be rather cautious in defining a single exponent characterizing the volatility behavior of the δD_{ice} series.

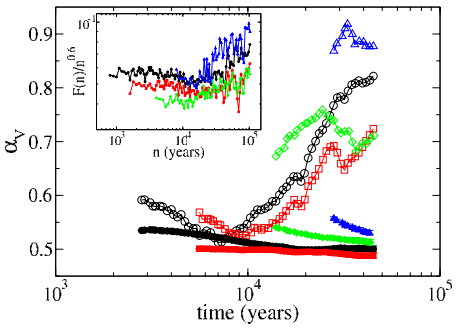

FIG. 6. (Color online) Local exponents α_V of the Vostok series shown as open symbols for resolutions R=100 yr (circles), 200 yr (squares), 500 yr (diamonds), and 1000 yr (triangles) obtained by DFA3. Closed symbols with error bars correspond to estimates obtained from 100 surrogates—see text for details. Inset: rescaled fluctuation functions of the Vostok series for the different R. Global fitting gives α_V=0.63, 0.61, 0.70, 0.85 for increasing R. For the surrogates, we find $\alpha_v = 0.51 \pm 0.03$, 0.50 ± 0.03, 0.53 ± 0.04, 0.55 ± 0.05 for increasing R.

To test whether the time series of the hydrogen isotope ratio is indeed nonlinear as proposed in Ref. [31], we generate surrogate data using the method described in Ref. [5]. This method preserves the linear properties of the $(\Delta \delta D_{ice})_j$ series but randomizes the Fourier phases which would contain all nonlinear properties. Thus, it effectively generates linear time series with the same distribution of increments and the same linear two-point correlations as the original one. Figure 6 shows a direct comparison between the local exponents α_V of the Vostok series and those of an ensemble of surrogates. The clear differences between the surrogates and the actual data for $R \geq 500$ yr allow us to reject the null hypothesis that the δD_{ice} series is linear. As follows from the inset of Fig. 6, the deuterium series is nonlinear over time scales of 5–100 kyr. This interval is slightly smaller than what was found previously when the influence of the uneven sampling was ignored [31].

Since δD_{ice} is a proxy for the temperature when the ice was formed, the findings imply that the variation in temperature over time scales between 5 and 100 kyr is nonlinear. To be more specific, the much higher value of α_V for the Vostok data compared to the surrogates indicates that there are nontrivial correlations in the volatility series. The presence of such correlations implies that subsequent values tend to be similar, i.e., values are clustered. Since volatility is a measure of the magnitude of a (temperature) change, it directly follows that each temperature change tends to be succeeded by a similar temperature change: large (small) temperature changes are followed by large (small) temperature changes as concluded in Refs. [31,32]. Note, however, that this result does not allow us to deduce any information regarding the *sign* of the changes.

To test whether the modified volatility series introduced in Sec. V for FBM allows one to obtain a better estimate for the volatility properties of the Vostok data as well, we first analyze the δD_{ice} series itself. In particular, it is necessary to estimate the behavior of the variance of the (stationary) increments as a function of the time interval, which is determined by the linear two-point correlation function of the

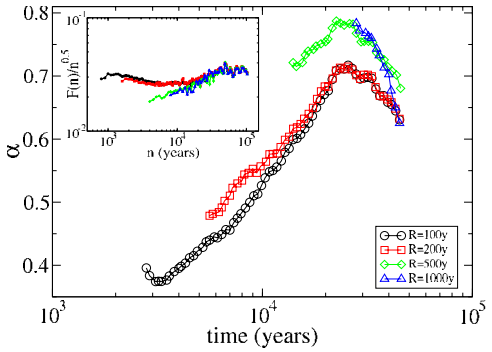

FIG. 7. (Color online) Local exponents α of the Vostok series for different resolutions R obtained by DFA3. Inset: respective rescaled fluctuation functions. Global fitting gives α=0.54, 0.59, 0.72, 0.72 for increasing R.

increments—see Eq. (A3)—or equivalently by the fluctuation function of the underlying time series [2]. As shown in the Appendix, if the linear two-point correlation function can be approximated by a power law one obtains an analogous expression to Eq. (9) where the exponent is identical to the exponent α given by the fluctuation function of the underlying time series.

Based on the results for FBM (see discussion of Fig. 2), we do not expect a strong influence of the uneven sampling for $R \geq 100$ yr on the estimate of the fluctuation function. This is confirmed by Fig. 7, which shows the fluctuation functions and the local exponents α. In contrast to FBM, though, there seems to be a systematic variation in the local exponents. This suggests that a single power law is too simplistic to capture the behavior of the fluctuation function of the Vostok series. Similar findings for other temperature proxies have been reported, for example, in Refs. [26,45].

The apparent absence of a single scaling exponent and the presence of nonlinearities in the δD_{ice} series as discussed above suggest that the applicability of the correction method using, for example, Eq. (9) could be limited in this case. This is indeed confirmed by Fig. 8, which shows the fluctuation function and the local exponents for the modified volatility series of δD_{ice}. Here, we have used the global values of α for

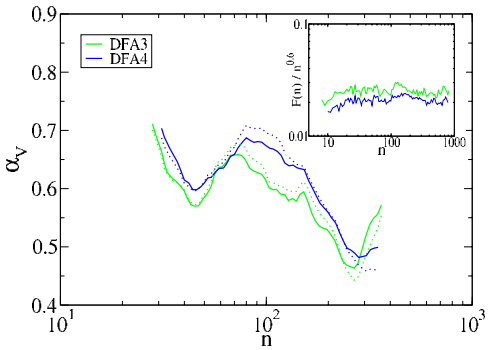

FIG. 8. (Color online) Local exponents α_V of the *modified* volatility series of the Vostok data using H=0.5 (solid lines) and 0.6 (dotted lines) in Eq. (9) for different DFA orders. The inset shows the respective rescaled fluctuation function for H=0.5 indicating that $\alpha_V \approx 0.6$ globally.

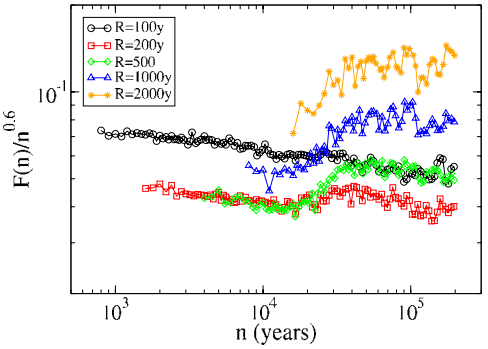

FIG. 9. (Color online) Rescaled fluctuation function of the EDC volatility series for different resolutions R obtained by DFA3. Global fitting gives α_V=0.53, 0.58, 0.70, 0.76, 0.74 for increasing R. For the surrogates (shown in Fig. 10), we find α_v =0.50±0.02, 0.50±0.02, 0.52±0.03, 0.53±0.04, 0.52±0.04 for increasing R.

R=100 and 200 yr given in Fig. 7 as guidance for selecting the exponent in Eq. (9). The obtained fluctuation functions can be approximated by a single $\alpha_V \approx 0.6$. This is significantly lower than the values for R=500 and 1000 yr in Fig. 6. Note also that resampling the data to a *minimal* resolution of up to 200 yr and then considering the modified volatility series does not change our findings significantly either [46]. This suggests that the nonlinearities—rather than the apparent absence of a single scaling exponent α—severely limit the applicability of the correction method in this case. This is supported by an analysis of nonlinear multifractal time series. For the integrated variant of the multiplicative random cascade process described in Ref. [43], we find that while on average the correct behavior is approximately recovered there are huge variations between realizations. This leads to much larger standard errors for the local and global exponents of the modified volatility series. For example, the standard error of the global α_V is about 0.2 clearly indicating that the predictive power of the modified volatility series is limited in this case.

VII. RESULTS FOR EPICA DOME C ICE CORE

While the Vostok ice core was the oldest ice core available for a number of years, the EPICA has recently provided another deep ice core at dome C, which extends much further back in time [15]. In particular, a high-resolution deuterium profile is now available covering the past 800 kyr [19]. Since it is expected that the δD_{ice} profile for the Vostok ice core and the EDC ice core share the same properties, we consider the latter one here as well.

Indeed, with very few exceptions, the properties of δD_{ice} data from the EDC ice core are consistent with those found for the Vostok data. For the volatility series, we observe again that the fluctuation function strongly varies with the chosen resolution—see Fig. 9. In an attempt to fit each function with a global α_V, we obtain values which are slightly less than those for the Vostok data. However, the variation in these global α_V's for $R \geq 500$ yr is much smaller for EDC than for Vostok. Moreover, it seems that the local exponents

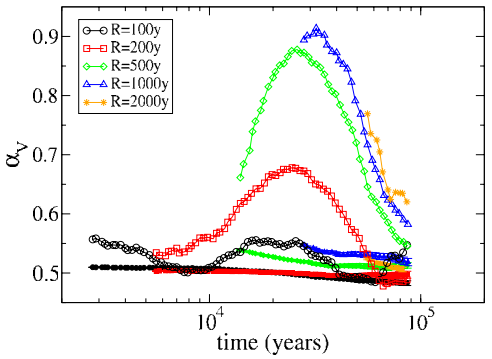

FIG. 10. (Color online) Local exponents α_V of the EDC series (open symbols) for different resolutions R corresponding to the fluctuation functions shown in Fig. 9. The curves with closed symbols and error bars correspond to estimates obtained from 100 surrogates—see text for details.

α_V follow a single function for $R \geq 500$ yr as Fig. 10 shows. This consistency gives us confidence that the results for $R \geq 500$ yr are reliable. Yet, it is important to notice that there are large fluctuations in the local values of α_V for any given resolution with $R \geq 500$ yr. This suggests that a simple power law with a single exponent is too simplistic to describe the fluctuation function of the volatility series.

As for the data from the Vostok ice core, the δD_{ice} data from the EDC ice core exhibit pronounced nonlinear behavior. Figure 10 shows a comparison between the local exponents α_V for the original data and an ensemble of surrogates. The clear differences between the surrogates and the actual data imply that we can reject the hypothesis that the deuterium series and, thus, the temperature series are linear. As follows from Fig. 9, the deuterium series is nonlinear over time scales between 5 and 200 kyr at least. This extends the results in Ref. [31].

VIII. DISCUSSION

By carefully analyzing the volatility properties of the deuterium series of the EDC ice core, we have been able to independently confirm and extend earlier results based on the Vostok ice core [31]: temperature changes over time scales between 5 and 200 kyr are clustered such that large changes tend to be followed by large changes, while small changes tend to be followed by small changes. These findings go well beyond the well-known glacial by interglacial variability dichotomy. Indeed, the observed long-range correlated temperature variations indicate not only that the Milankovitch periods of 20 and 40 kyr are secondary but also that contrary to common belief [47] climate dynamics of all time scales between 5 and 100 kyr are highly nonlinear. This important result provides a benchmark test for climate models and in particular rules out models which assume linear variations on those time scales. As shown in Ref. [32], many conceptual models proposed in the past fail this test, which has led to the conjecture that interaction between fast random fluctuations (representing atmospheric variability) and slowly varying fluctuations (representing oceanic variability) may underlie the observed nonlinearity. In addition, such a test is important to establish a clear connection between orbital variations and climate variations (see Ref. [48] for a discussion) and, thus, for ice core chronology.

Our results also show that a certain amount of care has to be taken in order to analyze time series that suffer from uneven sampling intervals. For FBM, one can correct for the induced biases in the volatility series by a simple rescaling approach, which should also be applicable to other stochastic processes. Nonlinearities can, however, limit the applicability of the method.

ACKNOWLEDGMENT

The authors thank Nicholas Watkins, Mervyn Freeman, Eric Wolff, and Regine Röthlisberger for stimulating discussions and support.

APPENDIX: CALCULATION OF THE VARIANCE

Let us consider a stationary signal u_i, where each u_i is a local time average of a continuously varying quantity $x(t)$ with zero mean, $u_i=[1/(t_{i+1}-t_i)]\int_{t_i}^{t_{i+1}}dt\int_0^t dt'\ x(t')$. Defining $n=t_{i+2}-t_{i+1}$ and $m=t_{i+1}-t_i$, it is straightforward to show that the difference between two subsequent values of u_i is given by

$$u_{i+1}-u_i=\int_0^{m+n} g(t)x(t)dt, \tag{A1}$$

where

$$g(t)=\begin{cases}\dfrac{t}{m} & \text{for } t\leq m\\ \dfrac{n+m-t}{n} & \text{for } t\geq m.\end{cases} \tag{A2}$$

To calculate the variance of $u_{i+1}-u_i$, we take advantage of the assumption that the mean of x is zero and we obtain

$$\begin{aligned}\mathrm{var}(u_{i+1}-u_i)&=\left\langle\int\int_0^{m+n} g(t_1)g(t_2)x(t_1)x(t_2)dt_1dt_2\right\rangle\\&=\int\int_0^{m+n} g(t_1)g(t_2)c(t_1-t_2)dt_1dt_2.\end{aligned} \tag{A3}$$

Here, $c(\tau)=\langle x_t x_{t+\tau}\rangle_t$ is the two-point correlation function of $x(t)$. It is straightforward to show that Eq. (A3) reduces to

$$\mathrm{var}(u_{i+1}-u_i)=\int_0^{m+n} h(\tau)c(\tau)d\tau, \tag{A4}$$

where h is given by

$$h(\tau) = \begin{cases} \dfrac{(n+m-\tau^3)}{12mn} + \dfrac{(n+m)(\tau-n)^3}{12mn^2} + \dfrac{(n+m)(\tau-m)^3}{12m^2n} & \text{for } 0 \le \tau \le n,m \\ \dfrac{(n+m-\tau)^3}{12mn} + \dfrac{(n+m)(\tau-n)^3}{12mn^2} & \text{for } m \le \tau \le n \\ \dfrac{(n+m-\tau)^3}{12mn} + \dfrac{(n+m)(\tau-m)^3}{12m^2n} & \text{for } n \le \tau \le m \\ \dfrac{(n+m-\tau)^3}{12mn} & \text{for } n,m \le \tau \le n+m. \end{cases} \tag{A5}$$

There are a number of special cases which are of particular interest. For the case of no correlations, i.e., $c(\tau)=\delta(\tau)$, Eq. (A4) evaluates as

$$\mathrm{var}(u_{i+1}-u_i) = h(0) = \frac{n+m}{6}. \tag{A6}$$

For the case of long-range correlations, i.e., $c(\tau)=|\tau|^{-\gamma}$, where $0<\gamma<1$, Eq. (A4) reduces to

$$\mathrm{var}(u_{i+1}-u_i) = \frac{\left(\dfrac{1}{mn}(m^3+n^3)(n+m)^{1-\gamma} - \dfrac{m+n}{mn}(m^{3-\gamma}+n^{3-\gamma}) + 3(n+m)^{2-\gamma}\right)}{(\gamma-4)(\gamma-3)(\gamma-2)(\gamma-1)} \tag{A7}$$

$$\approx \frac{(4-2^{\gamma})m^{2-\gamma}}{2^{\gamma}(\gamma-4)(\gamma-3)(\gamma-2)(\gamma-1)} \tag{A8}$$

where the last approximation is valid if $|n-m| \ll m/(2-\gamma)$ for all n and m. The expression is exact for $n=m$.

[1] P. Brockwell and R. Davis, *Time Series: Theory and Methods* (Springer Verlag, New York, 1987).
[2] H. Kantz and T. Schreiber, *Nonlinear Time Series Analysis* (Cambridge University Press, Cambridge, UK, 1997).
[3] P. Embrechts, C. Klüppelberg, and T. Mikosch, *Modelling Extremal Events for Insurance and Finance* (Springer, Berlin, 2004).
[4] *Time Series Analysis of Irregularly Observed Data*, Lecture Notes in Statistics Vol. 25, edited by E. Parzen (Springer, Berlin, 1983).
[5] T. Schreiber and A. Schmitz, Physica D **142**, 346 (2000).
[6] N. R. Lomb, Astrophys. Space Sci. **39**, 447 (1976).
[7] J. D. Scargle, Astrophys. J. **263**, 835 (1982).
[8] J. Koh and T. K. Sarkar, Digit. Signal Process. **15**, 44 (2005).
[9] W. Palma and N. H. Chan, J. Forecast. **16**, 395 (1997).
[10] M. Schulz and K. Stattegger, Comput. Geosci. **23**, 929 (1997).
[11] W. Palma and G. D. Pino, Biometrika **86**, 965 (1999).
[12] P. S. Wilson, A. C. Tomsett, and R. Toumi, Phys. Rev. E **68**, 017103 (2003).
[13] J. R. Petit *et al.*, Nature (London) **399**, 429 (1999).
[14] North Greenland Ice Core Project Members, Nature (London) **431**, 147 (2004).
[15] EPICA Community Members, Nature (London) **429**, 623 (2004).
[16] R. Spahni *et al.*, Science **310**, 1317 (2005).
[17] EPICA Community Members, Nature (London) **444**, 195 (2006).
[18] K. Kawamura *et al.*, Nature (London) **448**, 912 (2007).
[19] J. Jouzel *et al.*, Science **317**, 793 (2007).
[20] F. Lambert, B. Delmonte, J. R. Petit, M. Bigler, P. R. Kaufmann, M. A. Hutterli, T. F. Stocker, U. Ruth, J. P. Steffensen, and V. Maggi, Nature (London) **452**, 616 (2008).
[21] J. Pelletier and D. L. Turcotte, J. Hydrol. **203**, 198 (1997).
[22] E. Koscielny-Bunde, A. Bunde, S. Havlin, H. E. Roman, Y. Goldreich, and H. J. Schellnhuber, Phys. Rev. Lett. **81**, 729 (1998).
[23] A. A. Tsonis, P. J. Roebber, and J. B. Elsner, J. Clim. **12**, 1534 (1999).
[24] *Theory and Applications of Long-Range Dependence*, edited by P. Doukhan, G. S. Oppenheim, and M. S. Taqqu (Birkhäuser, Boston, USA, 2003).
[25] A. Bunde, J. F. Eichner, J. W. Kantelhardt, and S. Havlin, Phys. Rev. Lett. **94**, 048701 (2005).
[26] P. Huybers and W. Curry, Nature (London) **441**, 329 (2006).
[27] D. Rybski, A. Bunde, S. Havlin, and H. von Storch, Geophys. Res. Lett. **33**, L06718 (2006).
[28] A. Király, I. Bartos, and I. M. Jánosi, Tellus, Ser. A **58**, 593 (2006).
[29] Y. Ashkenazy, P. C. Ivanov, S. Havlin, Chung-K. Peng, A. L. Goldberger, and H. E. Stanley, Phys. Rev. Lett. **86**, 1900 (2001).
[30] R. B. Govindan, A. Bunde, and S. Havlin, Physica A **318**, 529 (2003).
[31] Y. Ashkenazy, D. R. Baker, H. Gildor, and S. Havlin, Geophys. Res. Lett. **30**, 2146 (2003).
[32] Y. Ashkenazy, D. R. Baker, and H. Gildor, J. Geophys. Res.

110, C02005 (2005).
[33] T. Kalisky, Y. Ashkenazy, and S. Havlin, Phys. Rev. E **72**, 011913 (2005).
[34] I. Bartos and I. M. Jánosi, Nonlinear Processes Geophys. **13**, 571 (2006).
[35] F. Wang, P. Weber, K. Yamasaki, S. Havlin, and H. E. Stanley, Eur. Phys. J. B **55**, 123 (2007).
[36] P. Embrechts and M. Maejima, *Selfsimilar Processes* (Princeton University Press, Princeton, NJ, 2002).
[37] Note that there are significant finite-size effects for $H \approx 0.75$. See Eq. (7) and Fig. 1 in Ref. [33].
[38] C. K. Peng, S. V. Buldyrev, S. Havlin, M. Simons, H. E. Stanley, and A. L. Goldberger, Phys. Rev. E **49**, 1685 (1994).
[39] J. Kantelhardt, E. Koscielny-Bunde, H. H. A. Rego, S. Havlin, and A. Bunde, Physica A **295**, 441 (2001).
[40] J. Davidsen (unpublished).
[41] To avoid the deviations for small n intrinsic to the DFA method, we employ the correction scheme based on random shuffling with 20 realizations introduced in Ref. [39].
[42] D. Maraun, H. Rust, and J. Timmer, Nonlinear Processes Geophys. **11**, 495 (2004).
[43] M. I. Bogachev, J. F. Eichner, and A. Bunde, Phys. Rev. Lett. **99**, 240601 (2007).
[44] Note that $c(\tau)$ is negative for $H < 0.5$.
[45] J. D. Pelletier, Earth Planet. Sci. Lett. **158**, 157 (1998).
[46] Directly using the estimate of the variance from Fig. 7 instead of applying Eq. (9) also had very limited success in improving the correction method.
[47] J. Imbrie *et al.*, Paleoceanography **7**, 701 (1992).
[48] M. E. Raymo and P. Huybers, Nature (London) **451**, 284 (2008).